Potential and Accurate Evaluation of Unmanned Aerial Vehicle Remote Sensing for Soil Surface Roughness Measurement

Lei Li, Xingming Zheng, *Member, IEEE*, Xiaofeng Li, *Member, IEEE*, Xiaojie Li, *Member, IEEE*, Tao Jiang, *Member, IEEE*, and Xiangkun Wan

***Abstract*—Soil surface roughness (SSR) plays an important role in the physical and hydrological processes of soil surfaces. In order to achieve nondestructive, fast, and large area measurement of SSR, unmanned aerial vehicle (UAV) photogrammetry method was used to take digital images at the altitude of 10 m on three plots and generated the digital elevation model for calculating SSR. From the results of UAV-based SSR, the following conclusions were obtained. First, the domain of soil surface height was consistent with the designed height of the three plots: smooth (all pixels: −5.5–6.5 cm and 80% pixels: −2.3–2.3 cm) < medium (all pixels: −8.5–8.5 cm and 80% pixels: −3.4–3.4 cm) < rough (all pixels: −16.0–13.0 cm and 80% pixels: −6.8–6.8 cm). Second, UAV-based SSR can represent their differences among the three plots, indicated by a consistent root-mean-square height (rmsh) and correlation length (cl) with the pin-profiler results. Third, UAV-based SSR results can reveal the anisotropy of SSR, and for the medium plot, the maximum variation of rmsh and cl with observed azimuth angle is 0.77 cm and 14.35 cm, respectively. The UAV-based SSR method has the advantages of low cost, high efficiency, and all-directional measurement, and can be used in remote sensing model and hydrological simulation.**

***Index Terms*—Correlation length, photogrammetry, root-mean-square height, soil surface roughness (SSR), unmanned aerial vehicle (UAV).**

I. Introduction

SOIL surface roughness (SSR) participates in surface physical and hydrological processes. It is an important index for describing the status of soil surface height and plays an important role in many processes, such as infiltration, runoff, detachment of soil due to water or wind, gas exchange, evaporation, and heat flux [1], [2]. SSR can not only represent the fluctuation degree of the soil surface but also is an important factor in remote sensing (optical and microwave) research. It can quantify the influence of the surface state on electromagnetic wave signal and then can be used to analyze the observation accuracy of reflectivity and radar backscattering coefficient [3], [6].

The methods of measuring SSR are mainly divided into contact type and noncontact type [7]. Contact methods include the pin-profiler method and chain method; noncontact methods include laser scanning, photogrammetry, and ultrasound [8]–[10]. Among them, the pin-profiler method has the advantages of easy operation and low cost, but it also has the disadvantages of destroying the surface state and limited representation. For example, the pin-profiler method was used to measure the SSR of the study area only from the direction perpendicular and parallel to the ridge. Moreover, the distance between the pins affects the measurement accuracy of SSR [11]. Laser scanning and ultrasonic measurement can obtain the highest accuracy results, but it is difficult to achieve large-scale observation because of the high requirements for the external environment. Ground photogrammetry can also obtain high-precision roughness parameters but limited by the photographic position, which can only measure small areas [12], [13]. For example, Gilliot *et al*. [14] used a camera to obtain point clouds in the range of 54 cm × 44 cm; Tao *et al*. [6] obtained point clouds in a circular area with a diameter of 92 cm. To obtain approximately 90% accuracy for the SSR, the length of the measured segment should be at least 40cl long and 200cl long, where cl is the mean surface correlation length [2], [4]. It can be found that the current SSR measurement methods may damage the soil surface, and the representativeness is limited. In order to solve the above problems and obtain a large area of high-precision soil surface height, unmanned aerial vehicle (UAV) photogrammetry provides a new idea for the measurement of SSR. The new method tackles the main limitations of the traditional methods, while the UAV can get SSR of the large area and many directions same with the ridge or different from the ridge on the surface. Moreover, some results have proved that the difference of digital surface model (DSM) between the UAV and terrestrial laser scanning was under ±1 cm [15], [16].

With the development of UAV, it is possible to obtain surface height [such as the surface slope, digital orthophoto map (DOM), DSM, and digital elevation model (DEM)] with horizontal resolution at millimeter or centimeter level [14]. UAV photogrammetry can acquire larger area and more directions of the SSR, and at the same time, can get the 3-D information of the soil surface, which is more accurate and comprehensive than the pin-profiler

Manuscript received April 17, 2021; revised June 8, 2021 and July 1, 2021; accepted July 27, 2021. Date of publication August 2, 2021; date of current version August 25, 2021. This work was supported by the National Key Research and Development Program of China and the National Natural Science Foundation of China under Grants 2018YFD1100101, 41971323 and 41771400. *(Corresponding author: Xingming Zheng.)*

Lei Li and Xiangkun Wan are with the Northeast Institute of Geography and Agroecology, Chinese Academy of Sciences, Changchun 130102, China, and also with the University of Chinese Academy of Sciences, Beijing 100049, China (e-mail: lilei@iga.ac.cn; wanxiangkun@iga.ac.cn).

Xingming Zheng, Xiaofeng Li, Xiaojie Li, and Tao Jiang are with the RS and GIS Center, Northeast Institute of Geography and Agroecology, Chinese Academy of Sciences, Changchun 130102, China (e-mail: zhengxingming@iga.ac.cn; lixiaofeng@iga.ac.cn; lixiaojie@iga.ac.cn; jiangtao@iga.ac.cn).

Digital Object Identifier 10.1109/JSTARS.2021.3101230

method and ground photogrammetry [10], [14]. Meanwhile, extract the slope of the soil surface from DEM, which is of great significance to the study of water infiltration, runoff, and so on [1]. Although UAV photogrammetry has the above advantages, there are also some problems (limited endurance and unstable positioning accuracy). Through flight experiments, this study analyzed whether the accuracy of UAV-based SSR can meet the application of remote sensing, hydrology, and soil erosion.

In this article, we focus on calculating the SSR of the farmland based on the UAV photogrammetry method. To achieve this objective, we used the UAV to take high spatial resolution images, obtain the DEM of each plot, and calculate the correlation length (cl) and root-mean-square height (rmsh). We validated the UAV-based SSR with the pin-profiler-based SSR to evaluate whether the UAV-based method was suitable to calculate SSR. Finally, we analyzed the anisotropy of SSR at different directions of the farmland surface. This method should be valuable in calculating more reliable and representative SSR for the application of remote sensing and hydrological model.

II. Materials and Methods

A. Experiments

The study area is located in the farmland area of Changchun city, Jilin province, Northeast China. The soil type of the experimental area is chernozem, with a soil organic content of 10 g/kg and soil bulk density of 1.03 g/cm^3. The percentages of sand, clay, and silt are 56, 12, and 32%, respectively. The study area is a temperate continental climate, and the rainfall is generally concentrated from June to August (400–800 mm/year) [11]. In order to study the feasibility of measuring microscale SSR by UAV photogrammetry, three bare soil surfaces were selected to carry out validation experiments, and the area of each plot was about 886 m^2. Among them, nontillage cultivation area was defined as smooth plot, ridge cultivation area was defined as medium plot, and ploughed farmland was defined as rough plot.

According to the area of each plot and the required spatial resolution (1.0 cm), set the flight parameters (overlap, flight altitude, speed, etc.) of the UAV and take digital images with the high-resolution camera carried by the UAV. In order to verify and analyze the accuracy of SSR calculated by UAV, measure the SSR by the pin-profiler method after each UAV flight. The pin profiler has a length of 1.1 m, with 110 needles and 1.0 cm interval. Place markers on the boundary of three plots to ensure the same position sampled by UAV and pin-profiler method (see Fig. 1). Measure the SSR of the marked position by pin profiler and digital camera on the ground, and vectorize in ArcGIS (ESRI, Redlands, California).

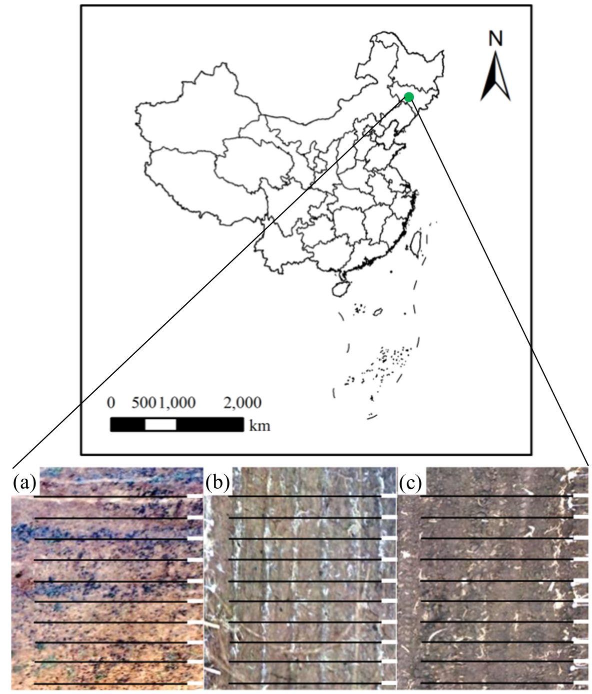

Fig. 1. Three soil surfaces with different roughness photographed on December 13, 2018. (a), (b), and (c) represent the smooth, medium, and rough plot, respectively; white rectangle represents the marker; black lines correspond to the white marker are the measurement location.

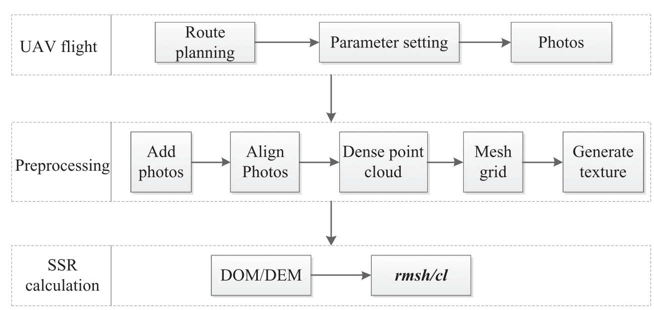

Fig. 2. Flowchart of UAV-image acquisition and processing.

B. UAV-Image Acquisition and Processing

This part includes the UAV flight, image preprocessing, and the calculation of SSR (see Fig. 2). Before the flight, the UAV flight route and the flight parameters were designed. Add the images acquired by UAV to image processing software and generate the DOM and DEM of each flight based on the process.

The UAV photogrammetry was performed on December 13, 2018, with a 12.4 megapixel Sony Exmor R CMOS camera equipped on DJI Inspire 1 Pro (DJI, Shenzhen, China), and its FOV was 94°. Before the flight, Altizure (Altizure, Shenzhen, China) was used to set the flight route, flight height (10 m), speed (2 m/s), and overlap (forward: 75% and side: 75%). Based on the above flight parameters, each flight time was 3 min, and the ground resolution of the image was 4.4 mm. Obtain 55 images in each plot and collect 165 images from three plots totally.

Then, the digital images acquired by UAV were processed by Agisoft Photoscan Profession Edition software (Agisoft LLC, St. Petersburg, Russia). Add the photos taken by UAV to the software, and the following processes were carried out in turn, align photo, build dense point cloud, build mesh grid, and generate texture (see Fig. 2). When processing the UAV image, the high-precision option was selected to align the photos; in the process of building dense point cloud, the high-quality option was selected; the dense point cloud was used as the data source to generate mesh; the adaptive orthophoto mapping mode was selected to generate texture. The generation of the point cloud is very important to obtain the height of each point and then calculate SSR. In this study, image features are identified as key points and, subsequently, matched by a scale-invariant feature transform algorithm between corresponding images to retrieve tie points. With the information of these homologous image points, the camera poses were calculated as well as the 3-D coordinates of the corresponding tie points, leading to a point cloud in an arbitrary coordinate system, via an iterative bundle adjustment [17], [18]. Finally, the DOM and digital elevation model (DEM) were the output. In this study, the DOM was used to identify the same position as the pin profiler measured. And then, the height value was extracted from DEM. Each plot was cropped to 40 m^2 (5 $\times$ 8 m), and the spatial resolution was resampled to 1.0 cm. The height was measured in the generated DEM, and then the value was used to calculate the SSR. In this study, in order to compare with the pin-profiler method and verify the feasibility of SSR measured by UAV, the UAV image was resampled.

C. Calculation Method of SSR

Root-mean-square height (rmsh) and correlation length (cl)

Roughness can be defined as a measure of the topographic relief of a surface [7]. In the field of microwave remote sensing, SSR was generally characterized by two parameters: root-mean-square height (rmsh) and correlation length (cl) [6], [8]. The rmsh and cl describe the SSR from the vertical and horizontal directions, respectively. Based on the DEM, extract the height value and then calculate the roughness parameters. The expression is

$$\mathrm{rmsh} = \sqrt{\sum\nolimits_{i=1}^{N} \left(z_i{}^2 - \bar{z}^2\right)/(N-1)} \tag{1}$$

where N is the number of height records, z_i is the height corresponding to record i, and $\bar{z}$ is the mean height of all the records. The spatial interval Δx between two adjacent sampling points should be less than 0.1λ (λ is the wavelength of the incident wave). A smaller Δx value is required for higher frequencies. The normalized experimental correlation function $R(h)$ for a 1-D surface profile $z(x)$ is defined as

$$R(h) = \left(\sum_{i=1}^{N(h)} z_i z_{i+h}\right) \Bigg/ \sum_{i=1}^{N} z_i{}^2 \tag{2}$$

where $R(h)$ is the experimental correlation function, which represents the correlation between height z of point i (z_i) and that of another point located at a lag distance h from it (z_{i+h}). $N(h)$ is the number of pairs considered in each lag h. The cl is then defined arbitrarily as h when $R(h) = 1/e$. Here, the cl of a surface provides a reference for estimating the statistical independence of two points on the surface. If two points are separated by a horizontal distance greater than cl, then their heights can be considered to be (approximately) statistically independent of one another. In the extreme case of a perfectly smooth (specular) surface, every point on the surface is correlated with every other point with a correlation coefficient of unity. In this case, cl = ∞ [11], [19].

Methodology for obtaining UAV-based and pin-profiler-based SSR

Based on the DEM acquired by the UAV image, extract the height values of the marked position. Furthermore, this study only analyzed the feasibility and accuracy of the UAV photogrammetry method to obtain rmsh and cl, so fit the slope trend of the plot based on the height values, and then eliminate the slope. The average height of each plot was uniformly subtracted from the height values without changing the surface relative height change, and the height values distributed around zero were obtained. In order to ensure the consistency with the pin-profiler method, extract 330 height values from the DEM acquired by UAV in the calculation of each roughness parameter.

In the field measurement, there might be periodicity fluctuation or slope on the farmland surface in the real situation. Therefore, in order to accurately describe the SSR, three groups of image data must be continuously acquired along the same direction, and three groups of images should be fused (head and tail joined) as one result [11]. Based on the above method, ten groups of images were acquired and every three end-to-end images were combined as one group. Then, the images acquired by the pin profiler and digital camera on the ground were vectorized in ArcGIS, and the vector position in each image was described. Finally, use the vectorization image to calculate the SSR.

In order to analyze the anisotropic characteristics of SSR, extract UAV-based height from different azimuth angles of the soil surface. In this study, 0° and 180° represent the direction of the ridge, and 90° represent the direction perpendicular to the ridge along the ground. The angle between the ridge direction and observation direction was set to 0–180°, with an interval of 10°. In each direction, extract the height values from DEM and then the SSR was calculated.

D. Accuracy Evaluation of UAV-Based SSR

In order to quantitatively evaluate the roughness based on UAV photogrammetry, the correlation coefficient (R), root-mean-square error (RMSE), and the average deviation (Bias) were calculated by taking the observation results of the pin-profiler method as reference data. The expressions are as follows:

$$\mathrm{R} = \frac{\frac{1}{N}\sum_{i=1}^{N}\left(M_i - \bar{M}\right)\left(O_i - \bar{O}\right)}{\sqrt{\frac{1}{N}\sum_{i=1}^{N}\left(M_i - \bar{M}\right)^2}\sqrt{\frac{1}{N}\sum_{i=1}^{N}\left(O_i - \bar{O}\right)^2}} \tag{3}$$

$$\mathrm{RMSE} = \sqrt{\frac{1}{N}\sum\nolimits_{i=1}^{N}\left(M_i - O_i\right)^2} \tag{4}$$

$$\mathrm{Bias} = \frac{1}{N}\sum\nolimits_{i=1}^{N}\left(M_i - O_i\right) \tag{5}$$

where M_i and O_i are the UAV-based and pin-profiler-based SSR (rmsh and cl), respectively. $\bar{M}$ and $\bar{O}$ represents the average of M_i and O_i, respectively.

III. Results

A. DEM of Three Plots From UAV Measurement

According to the DEM obtained by UAV photogrammetry, the normalized heights around zero were obtained [see Fig. 3(a)–(c)]. The height domain of the smooth plot was the smallest (−5.5–6.5 cm), and the domain of the medium plot was in the middle (−8.5–8.5 cm), while the domain of the rough plot was the largest (−16.0–13.0 cm). The statistical histogram of the height conforms to the characteristics of normal distribution. Based on Fig. 3(d)–(f), pixels in the domain of −2.3–2.3 cm,

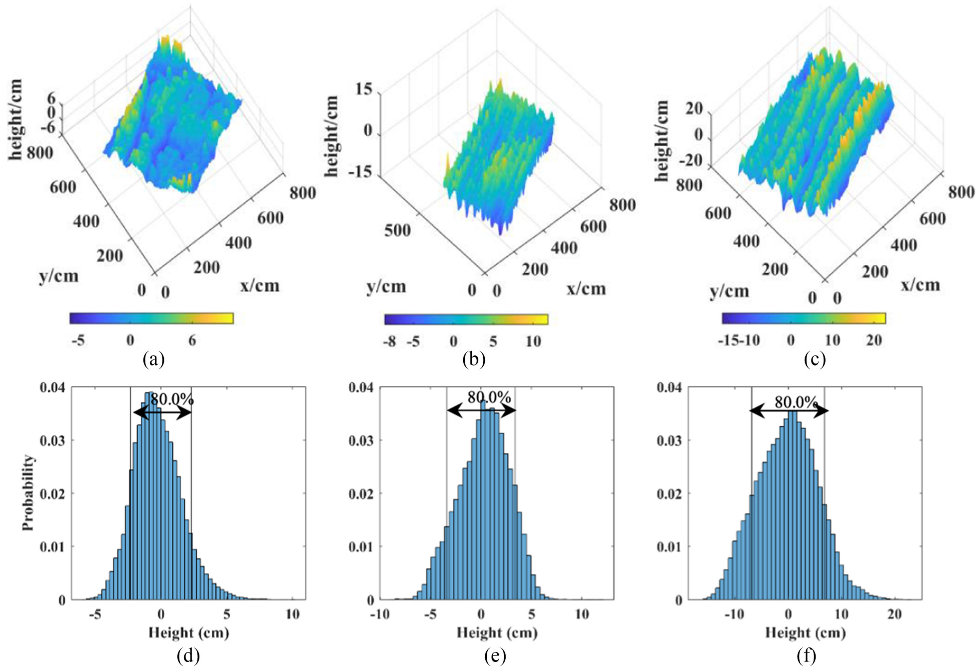

Fig. 3. UAV-based DEM results of the three plots and their histogram of the surface height. (a) and (d) for the smooth plot. (b) and (e) for the medium plot. (c) and (f) for the rough plot.

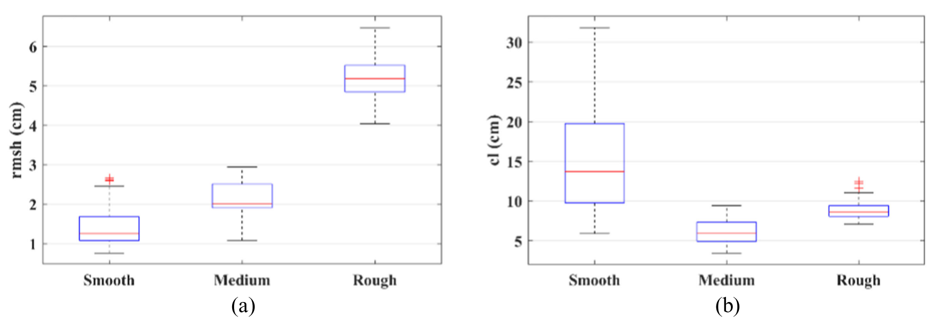

Fig. 4. Boxplot of UAV-based (a) rmsh and (b) cl of three roughness plots (smooth, medium, and rough).

-3.4–3.4 cm, and -6.8–6.8 cm accounted for 80.0% of the three plots of smooth, medium, and rough, respectively.

Fig. 4(a) showed that the UAV-based rmsh increased gradually from smooth plot to medium plot and then to the rough plot on the ridge direction. Although cl did not show a significant increasing or decreasing trend, the cl in the smooth plot was larger than that of the other two plots. Furthermore, in the boxplot of cl, the smooth plot had the greatest discrete degree, while the other two plots performed well.

TABLE I
COMPARISON OF UAV-BASED AND PIN-PROFILER-BASED SSR

	rmsh			cl		
	R	RMSE	Bias	R	RMSE	Bias
Smooth	0.15	0.46	-0.30	-0.70	7.42	4.02
Medium	0.66	0.37	-0.66	0.10	1.54	-6.28
Rough	0.17	0.49	-0.59	-0.22	1.19	-4.08
Mean	0.99	0.54	-0.52	-0.60	4.91	-2.11

Mean represents the three rough surfaces calculated comprehensively.

B. Comparison of rmsh and cl Results From UAV and Pin-Profiler Method

Fig. 5(a) showed that the value of rmsh is distributed near the 1:1 line, and Fig. 5(c) showed that the average rmsh value of the three plots is increased from smooth to rough plot. Furthermore, the fitted line of the rmsh is close to the 1:1 line, and the standard deviation was small. Table I presented that the correlation coefficient of average rmsh between the pin profiler and UAV was 0.99 for all three plots, which indicated that the UAV-based method had good performance in representing the rmsh. Fig. 5(b) showed that the distribution of cl was discrete, and the fitted line based on the mean value was far from the 1:1 line [see Fig. 5(d)]. In order to analyze the performance of the UAV-based method in each plot, the R, RMSE, and Bias were calculated (see Table I). The rmsh of the medium plot had the best correlation among the three plots ($R = 0.66$), while the

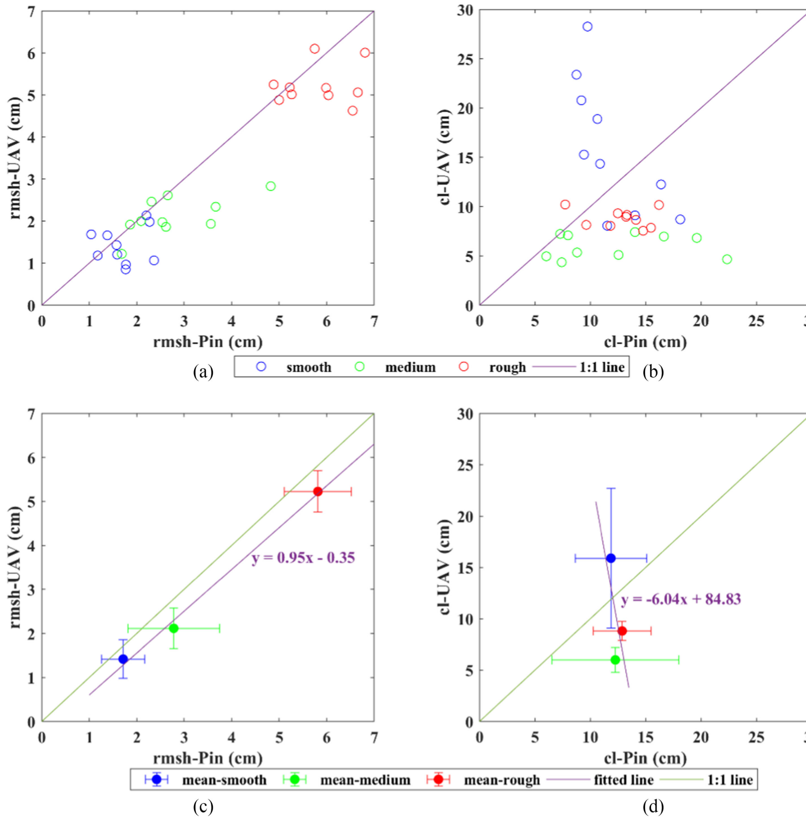

Fig. 5. Scatter of UAV-based and pin-profiler-based roughness results at three plots. [(a) and (c) represent the rmsh and average rmsh, respectively, (b) and (d) represent the cl and average cl, respectively; blue circle represents the smooth plot, green circle represents the medium plot, and red circle represents the rough plot).

other two plots had poor correlation (see Table I). And there was no significant correlation between the two methods about cl [see Fig. 5(b)]. Nevertheless, the cl value of the smooth plot was the largest dynamic domain among the three plots. The cl of the medium and rough plots showed that the result of UAV photogrammetry was more stable than that of the pin-profiler method. The cl of the three plots measured by the pin-profiler method was very close (smooth: 11.9 cm; medium: 12.3 cm; rough: 12.9 cm).

The error analysis of cl showed that there was uncertainty in the UAV photogrammetry method, and the average RMSE was 4.91 cm. In addition, the average Bias of rmsh was very small (about −0.52 cm), and the average Bias of cl was only −2.11 cm for all of the three plots (see Table I).

C. Anisotropy of Surface rmsh and cl Derived From UAV Photogrammetry

In this study, the medium plot was consistent with those of the dry farmland in Northeast China, and the change of rmsh and cl at different directions was analyzed, and the results were shown in Fig. 6.

The rmsh was approaching the minimum at 0° and 180°, that is, rmsh in the direction of the ridge was the minimum (1.95 cm) [see Fig. 6(a)]. Moreover, the maximum of the rmsh was in the direction of 20° and 160°, and the value was 2.72 cm. Therefore, the maximum rmsh difference on different azimuth angles was 0.77 cm for the medium plot. However, the cl had the opposite relationship with rmsh, and its value in 10° and 170° was close to the peak (19.88 cm). Furthermore, the minimum of the cl was in the direction of 70° and 110°, and the value was 5.53 cm. Consequently, the maximum difference on different azimuth angles was 14.35 cm for the medium plot. As the angle between the sampling direction and ridge direction increased, the rmsh increased, while the cl decreased.

IV. Discussion

A. Application Potential of UAV-Based SSR

As an observation technology between the satellite and ground, UAV remote sensing has begun to play an important role in agriculture, forestry, engineering, and other fields. In the research of SSR, UAV can quickly obtain high-precision and large-scale roughness parameters based on its advantages of high spatial resolution, low cost, and good real-time performance. Meanwhile, UAV could obtain the height information of 3-D surface, then topography, slope, and the exact profile of surface geometry can be captured. UAV could measure the SSR of field scale, while the pin-profiler method could only measure roughness parameters on the ground surface in one direction per time [20]. In remote sensing observation, a given surface may "appear" very rough to an optical wave, but it may "appear" very smooth to a microwave [21]. Under this background, the images acquired by UAV could be resampled in accordance with the research objective so that the SSR or microtopography on different spatial scales can be measured. Furthermore, SSR

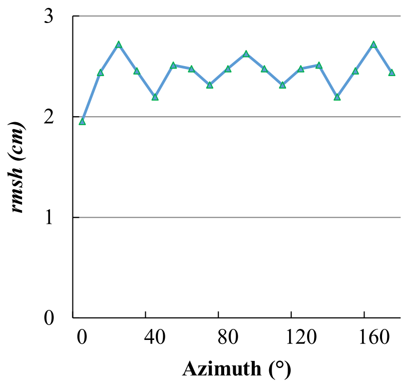

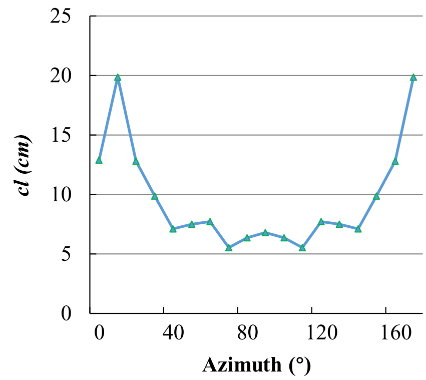

Fig. 6. Variation of UAV-based (a) rmsh and (b) *cl* at different directions.

reflects the fluctuation state of aggregates on the soil surface and also indicates the area of soil in contact with the external environment (air and sunshine), which is very important for reflecting the ability of soil surface evaporation.

B. Reliability of UAV-Based SSR

There are some limitations when a UAV acquires the height change characteristics of the plot, such as positioning accuracy, altitude, and camera resolution. Due to the difference in positioning accuracy, resulting from the number of global position satellites, the accuracy of the DEM may be affected. However, the measurement accuracy of UAV photogrammetry technology can still reach subcentimeters level [14], [22]. Although the rmsh based on UAV and pin-profiler method had a good correlation (0.99), and the cl between the two methods is poor (−0.60). Previous studies have shown that the calculation of cl needs a long sampling length [4], so the accuracy of the pin-profiler method would be limited. UAV has the advantage of measuring SSR in a large area and will play an important role in the research of soil erosion, remote sensing inversion, and hydrological interaction in the future.

C. Anisotropy of UAV-Based SSR

In optical remote sensing, SSR is related to the bidirectional reflectance distribution function, which affects the estimation of reflectance. In microwave remote sensing, with high precision and large area of SSR acquired by UAV, the multidirectional and accurate results can be used in soil moisture retrieval. In the field of radar remote sensing, the effect of SSR on the backscattering coefficient could not be ignored. Previous studies have shown that the variation of observation direction and SSR may lead to the deviation of the backscattering coefficient as high as 20 dB [21]. Therefore, it is necessary to study the anisotropy of SSR. In this study, the anisotropy of SSR was analyzed. The difference of SSR in each direction was obvious (rmsh: 0.77 cm and cl: 14.35 cm), which provided a basis for estimating soil surface parameters and remote sensing model application [6].

V. Conclusion

This article investigated the feasibility and accuracy of SSR measured by the UAV photogrammetry method by designing comparative observation of different surface roughness (smooth, medium, and rough). By comparing the roughness results of UAV and pin profiler, the following conclusions were obtained.

1) The change of soil surface height measured by UAV was consistent with the real surface. UAV photogrammetry method can not only avoid damaging the surface but also with the ability to measure SSR in a large area.
2) The UAV-based SSR was consistent with the pin-profiler-based SSR. The correlation of rmsh measured by the two methods was high, and their correlation of cl was low, which may be due to the limited sampling length of the pin profiler.
3) UAV photogrammetry method could quickly acquire SSR over wide areas, which can be used for anisotropic analysis, and the cost is low.

UAV-based DEM can be employed to estimate SSR in any azimuth direction and reveal the ridge characteristics of the soil surface, which can serve for establishing the land surface parameters retrieval model based on the high spatial resolution radar data.

References

[1] C.-H. Huang and J. M. Bradford, “Applications of a laser scanner to quantify soil microtopography,” *Soil Sci. Soc. Amer. J.*, vol. 56, no. 1, pp. 14–21, 1992, doi: 10.2136/sssaj1992.03615995005600010002x.

[2] X. Zheng, K. Zhao, X. Li, Y. Li, and J. Ren, “Improvements in farmland surface roughness measurement by employing a new laser scanner,” *Soil Tillage Res.*, vol. 143, pp. 137–144, 2014, doi: 10.1016/j.still.2014.06.010.

[3] T. M. Zobeck and C. A. Onstad, “Tillage and rainfall effects on random roughness: A review,” *Soil Tillage Res.*, vol. 9, no. 1, pp. 1–20, 1987, doi: 10.1016/0167-1987(87)90047-X.

[4] Y. Oh and Y. C. Kay, “Condition for precise measurement of soil surface roughness,” *IEEE Trans. Geosci. Remote Sens.*, vol. 36, no. 2, pp. 691–695, Mar. 1998.

[5] N. E. C. Verhoest, H. Lievens, W. Wagner, J. Alvarez-Mozos, M. S. Moran, and F. Mattia, “On the soil roughness parameterization problem in soil moisture retrieval of bare surfaces from synthetic aperture radar,” *Sensors*, vol. 8, no. 7, pp. 4213–4248, 2008, doi: 10.3390/s8074213.

[6] H. Tao, Q. Chen, Z. Li, J. Zeng, and X. Chen, “Improvement of soil surface roughness measurement accuracy by close-range photogrammetry,” *Trans. Chin. Soc. Agricultural Eng.*, vol. 33, no. 15, pp. 162–167, 2017, doi: 10.11975/j.issn.1002-6819.2017.15.021.

[7] F. Bretar, M. Arab-Sedze, J. Champion, M. Pierrot-Deseilligny, E. Heggy, and S. Jacquemoud, “An advanced photogrammetric method to measure surface roughness: Application to volcanic terrains in the Piton de la Fournaise, Reunion Island,” *Remote Sens. Environ.*, vol. 135, pp. 1–11, 2013, doi: 10.1016/j.rse.2013.03.026.

[8] X. Zheng, K. Zhao, and X. Li, “Accuracy analysis of agriculture soil surface roughness parameter,” *J. Geo-Inf. Sci.*, vol. 15, no. 5, pp. 752–760, 2013, doi: 10.3724/SP.J.1047.2013.00752.

[9] T. Bauer, P. Strauss, M. Grims, E. Kamptner, R. Mansberger, and H. Spiegel, “Long-term agricultural management effects on surface roughness and consolidation of soils,” *Soil Tillage Res.*, vol. 151, pp. 28–38, 2015, doi: 10.1016/j.still.2015.01.017.

[10] I. V. Florinsky and D. P. Bliakharskii, “The 2017 catastrophic subsidence in the Dålk Glacier, East Antarctica: Unmanned aerial survey and terrain modelling,” *Remote Sens. Lett.*, vol. 10, no. 4, pp. 333–342, 2019, doi: 10.1080/2150704X.2018.1552810.

[11] X. Zheng, L. Li, S. Chen, T. Jiang, X. Li, and K. Zhao, “Temporal evolution characteristics and prediction methods of spatial correlation function shape of rough soil surface,” *Soil Tillage Res.*, vol. 195, 2019, Art. no. 104417, doi: 10.1016/j.still.2019.104417.

[12] M. K. Shepard and B. A. Campbell, “Shadows on a planetary surface and implications for photometric roughness,” *Icarus*, vol. 134, no. 2, pp. 279–291, 1998, doi: 10.1006/icar.1998.5958.

[13] R. G. Moreno, A. Saa Requejo, A. M. Tarquis Alonso, S. Barrington, and M. C. Díaz, “Shadow analysis: A method for measuring soil surface roughness,” *Geoderma*, vol. 146, no. 1/2, pp. 201–208, 2008, doi: 10.1016/j.geoderma.2008.05.026.

[14] J. M. Gilliot, E. Vaudour, and J. Michelin, “Soil surface roughness measurement: A new fully automatic photogrammetric approach applied to agricultural bare fields,” *Comput. Electron. Agriculture*, vol. 134, pp. 63–78, 2017, doi: 10.1016/j.compag.2017.01.010.

[15] A. Eltner, P. Baumgart, H.-G. Maas, and D. Faust, “Multi-temporal UAV data for automatic measurement of rill and interrill erosion on loess soil,” *Earth Surf. Processes Landforms*, vol. 40, no. 6, pp. 741–755, 2015, doi: 10.1002/esp.3673.

[16] M. Milenković, W. Karel, C. Ressl, and N. Pfeifer, “A comparison of UAV and TLS data for soil roughness assessment,” *ISPRS Ann. Photogramm. Remote Sens. Spatial Inf. Sci.*, vol. 3–5, pp. 145–152, 2016.

[17] M. R. James, S. Robson, S. d’Oleire-Oltmanns, and U. Niethammer, “Optimising UAV topographic surveys processed with structure-from-motion: Ground control quality, quantity and bundle adjustment,” *Geomorphology*, vol. 280, pp. 51–66, 2017, doi: 10.1016/j.geomorph.2016.11.021.

[18] N. Onnen, A. Eltner, G. Heckrath, and K. van Oost, “Monitoring soil surface roughness under growing winter wheat with low-altitude UAV sensing: Potential and limitations,” *Earth Surf. Process Landforms*, vol. 45, pp. 3747–3759, 2020, doi: 10.1002/esp.4998.

[19] F. T. Ulaby, P. P. Batlivala, and M. C. Dobson, “Microwave backscatter dependence on surface roughness, soil moisture, and soil texture: Part I—Bare soil,” *IEEE Trans. Geosci. Electron.*, vol. 16, no. 4, pp. 286–295, Oct. 1978.

[20] G. Pardini, “Fractal scaling of surface roughness in artificially weathered smectite-rich soil regoliths,” *Geoderma,* vol. 117, no. 1/2, pp. 157–167, 2003, doi: 10.1016/S0016-7061(03)00164-2.

[21] F. T. Ulaby *et al.*, *Microwave Radar and Radiometric Remote Sensing*. Ann Arbor, MA, USA: Univ. Michigan Press, 2014.

[22] X. Zheng, T. Jiang, X. Li, Y. Ding, and K. Zhao, “The temporal variation of farmland soil surface roughness with various initial surface states under natural rainfall conditions,” *Soil Tillage Res.,* vol. 170, pp. 147–156, 2017, doi: 10.1016/j.still.2017.03.015.

Lei Li received the master’s degree in surveying and mapping engineering from the College of Geo-Exploration Science and Technology, Jilin University, Changchun, China, in 2018. He is currently working toward the Ph.D. degree in cartography and geographical information system with the Northeast Institute of Geography and Agroecology, Chinese Academy of Sciences, Changchun, China.

His research interests include agricultural remote sensing, hydrological models, data assimilation, and unmanned aerial vehicle agricultural remote sensing.

Xingming Zheng (Member, IEEE) received the Ph.D. degree in cartography and geographic information system from the Northeast Institute of Geography and Agroecology, Chinese Academy of Sciences, Changchun, China, in 2012.

Since July 2012, he has been a Research Associate with the Northeast Institute of Geography and Agroecology, Chinese Academy of Sciences. His research interests include passive microwave remote sensing of soil moisture, geophysical inversion model, microwave radiative/scattering transfer model, and its application on crop canopy.

Xiaofeng Li (Member, IEEE) received the B.S. and M.S. degrees in mathematics from Jilin University, Changchun, China, in 2002 and 2005, respectively, and the Ph.D. degree in remote sensing and geosciences from the Chinese Academy of Sciences, Changchun, China, in 2008.

He is currently a Professor with the Research Center of Remote Sensing and Geoscience, Northeast Institute of Geography and Agroecology, Chinese Academy of Sciences.

His current research interests include land surface parameters inversion by remote sensing data, image processing, and data analysis. He has authored or coauthored more than 50 papers in journals and conference proceedings.

Li is also the Chair of the IEEE GRSS Changchun Chapter.

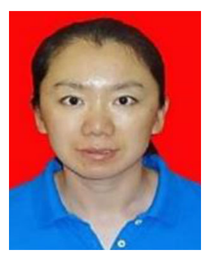

Xiaojie Li (Member, IEEE) received the Ph.D. degree in optical engineering from Tianjin University, Tianjin, China, in 2010.

Her major fields of study mainly include photoelectric detection technology, remote sensing data processing, and high-performance computing. She is currently an Associate Professor with the Northeast Institute of Geography and Agroecology, Chinese Academy of Sciences, Changchun, China. Her current interests include remote sensing data processing and high-performance computing.

Tao Jiang (Member, IEEE) received the Ph.D. degree in cartography and geographic information system from the Northeast Institute of Geography and Agroecology, Chinese Academy of Sciences, Changchun, China, in 2019.

He is currently an Engineer with Microwave Remote Sensing and Geoscience, Northeast Institute of Geography and Agroecology, Chinese Academy of Sciences. His research involves microwave radiometer design and development, and detection of radio frequency interference.

Xiangkun Wan received the bachelor’s degree in electronic and information engineering from Jilin University, Changchun, China, in 2015. He is currently working toward the Ph.D. degree in cartography and geographical information system with the Northeast Institute of Geography and Agroecology, Chinese Academy of Sciences, Changchun, China.

His research interests include microwave radiometer design and drone-borne radiometer design.